



Modification of electrospun PVA/PAA scaffolds by cold atmospheric plasma: alignment, antibacterial activity, and biocompatibility

Nehir Arik¹ · Alper Inan² · Fatma Ibis³ · Emine A. Demirci³ · Ozan Karaman^{3,4} · Utku K. Ercan^{3,4} · Nesrin Horzum^{1,5} 

Received: 21 November 2017 / Revised: 18 May 2018 / Accepted: 19 June 2018 /
Published online: 23 June 2018
© Springer-Verlag GmbH Germany, part of Springer Nature 2018

Abstract

The ongoing search for better antibacterial wound care dressings has led to the design and fabrication of advanced functional nanomaterials. Taking advantage of electrospinning and cold atmospheric plasma (CAP), free-standing nanofibrous scaffolds are promising for use in novel biomedical applications. Random and aligned polyvinyl alcohol (PVA)/polyacrylic acid (PAA) nanofiber scaffolds are fabricated by electrospinning and treated with CAP. In this study, we investigate the effects of CAP treatment on alignment, hydrophilicity, antibacterial activity, and biocompatibility in determining the surface properties of the nanofibrous scaffolds. The results of vibrational polarization spectroscopy analysis indicate that CAP treatment changes the degree of alignment of the nanofibers. Furthermore, both random and aligned CAP-treated nanofibrous scaffolds show significant antibacterial activity against the *E. coli* strain. The results of an in vitro scratch assay reveal that CAP treatment of PVA/PAA nanofibers has no toxic effect.

Keywords Alignment · Cold atmospheric plasma · Electrospinning · Nanofibrous scaffold

Introduction

The design and fabrication of scaffolds have attracted widespread interest in biomaterials research fields such as tissue engineering and drug delivery. In the selection of ideal scaffold materials, the chemical (i.e., hydrophilicity, surface charge

Electronic supplementary material The online version of this article (<https://doi.org/10.1007/s00289-018-2409-8>) contains supplementary material, which is available to authorized users.

✉ Nesrin Horzum
nesrin.horzum.polat@ikc.edu.tr

Extended author information available on the last page of the article

density, free energy, surface chemical groups), physical (i.e., porosity, permeability, surface area, topography, mechanical integrity), and biochemical (i.e., antimicrobial property, biodegradability, biocompatibility) aspects must be considered [1]. For instance, the antimicrobial property can be confined to the surface of the scaffolds, with surface modification achieved via changes in the chemistry, morphology, or deposition of specific nanoparticles such as silver or copper. However, introducing an antimicrobial agent into a biomaterial may affect its stability or processability [2]. To overcome these advantages, researchers have recently given special attention to the utilization of cold atmospheric plasma (CAP) for providing materials with antimicrobial properties.

Plasma, considered to be the fourth state of matter, consists of charged particles, electrons, photons, and free radicals that can readily react with microorganisms [3]. By virtue of these interactions, microorganisms can be inactivated in a controlled area. This cost-effective and environmentally friendly technique also noticeably alters surface properties, including the material's hydrophilicity and biocompatibility [4, 5]. Numerous synthetic and natural polymers have been used in CAP technology, including chitosan [6–10], polycaprolactone [11–13], poly(lactic acid) [14], poly(lactic acid-co-glycolic acid) [15], poly(vinyl alcohol) [4, 16], and polyurethane [17] in the form of gels [18, 19], nanoparticles [11, 20], and electrospun nanofibers [21, 22]. Of these, the electrospun fibrous scaffolds can be especially interesting due to their flexibility, high surface-to-volume ratio, porosity, and structural characteristics [23, 24].

The contributions of CAP to electrospun fibers include not only enhanced surface hydrophilicity and functionalization, but also incremental improvements in mechanical strength and crystallinity [25–27]. In addition, the CAP treatment of pre-electrospinning solutions has been reported to be an advantageous strategy for obtaining finer and bead-free nanofibers [28]. Shi et al. [5] showed that CAP treatment enhanced the electrospinnability of polyethylene oxide solutions. The authors also demonstrated a speculative diagram for the alignment of a CAP-treated polymer solution along the direction of the electrical field during the electrospinning process. Since the pioneering experiments on the CAP treatment of the properties of pre-electrospinning solutions, we have focused on investigating the effects of CAP treatment on the alignment, antibacterial activity, and biocompatibility of nanofibrous scaffolds. In doing so, a PVA/PAA blend solution was used as a model since it is water adsorbable, electrospinnable, and intermolecular thermo-cross-linkable via an ester linkage between the hydroxyl group of PVA and the carboxyl group of PAA [29]. In addition, we realize an increased alignment of the charged polymer chains along the electrical field during electrospinning followed by CAP treatment. We propose a green strategy that uses a combination of water-based electrospinning (without the use of any toxic cross-linking reagents) and CAP treatment for the fabrication of nanofibrous scaffolds for use in wound dressings, tissue engineering, and food packaging.

Experimental

Materials

Polyvinyl alcohol (PVA, $M_n \sim 30,000\text{--}70,000 \text{ g mol}^{-1}$, 87–90% hydrolyzed) and polyacrylic acid (PAA, $M_w \sim 450,000 \text{ g mol}^{-1}$) were received from Sigma-Aldrich and used them without further purification. Trypticase soy broth (TSB) and trypticase soy agar (TSA) used in microbiological tests were purchased from Sigma-Aldrich, and phosphate-buffered saline (PBS) used in the dilution of organisms was purchased from Biowest. We obtained L929 fibroblast cells from the Ege University Research Group of the Animal Cell Culture and Tissue Engineering Laboratory. We routinely cultured the cells at 37 °C in a 5% CO₂-humidified atmosphere in Dulbecco's Modified Eagle's Medium (Sigma-Aldrich, St. Louis, Missouri, USA), supplemented with 2 mM of L-glutamine, 20 U/mL of penicillin–streptomycin (Genaxxon BioScience, Ulm, Germany), and 10% heat-inactivated fetal bovine serum (FBS; Sigma-Aldrich, Steinheim, Germany). Deionized water treated with plasma and ultrapure water used in the experiments as needed was obtained from a Merck Millipore Direct-Q® 3 UV Water Purification System.

Preparation of the electrospinning solutions

Figure 1 shows a schematic diagram for the fabrication of the PVA/PAA nanofiber scaffolds and CAP setup. Two sets of PVA/PAA electrospinning solutions were prepared by using distilled water (DW) and plasma-treated water (PT-DW). CAP treatment of the water was performed for 3 min, as described in [30]. Briefly, 1 mL of deionized water was transferred into a custom-made glass fluid holder and placed it under a custom-made dielectric barrier discharge (DBD) plasma electrode while maintaining 2 mm of discharge gap. DBD plasma electrode was connected to an alternating current (AC)-powered microsecond pulsed power source to generate plasma at a voltage of 31 kV, a frequency of 1.5 kHz, and pulse duration of 5 μs to yield about 0.28 W/cm² of power distribution. PVA solution was prepared by dissolving PVA (0.696 g) in water for 3 h by magnetic stirring. Then, the PVA solution was added to an 8 wt% aqueous solution of PAA (0.260 g), and the mixture was stirred for 2 h at room temperature. The total polymer concentration of the mixture was 10 wt %.

Fabrication of the PVA/PAA nanofiber scaffolds

The electrospinning experiments were conducted on a commercial platform (Inovenso Basic Setup) covered with a plexiglass box to ensure safety and prevent any disturbances from air convection. The viscous solutions of PVA/PAA were loaded into a 5-mL plastic syringe. The positive electrode was applied to the spinneret and an aluminum foil was used as a counter electrode. A potential of 12.5 kV was applied at a tip-to-collector distance of 21 cm, and the electrospinning time was

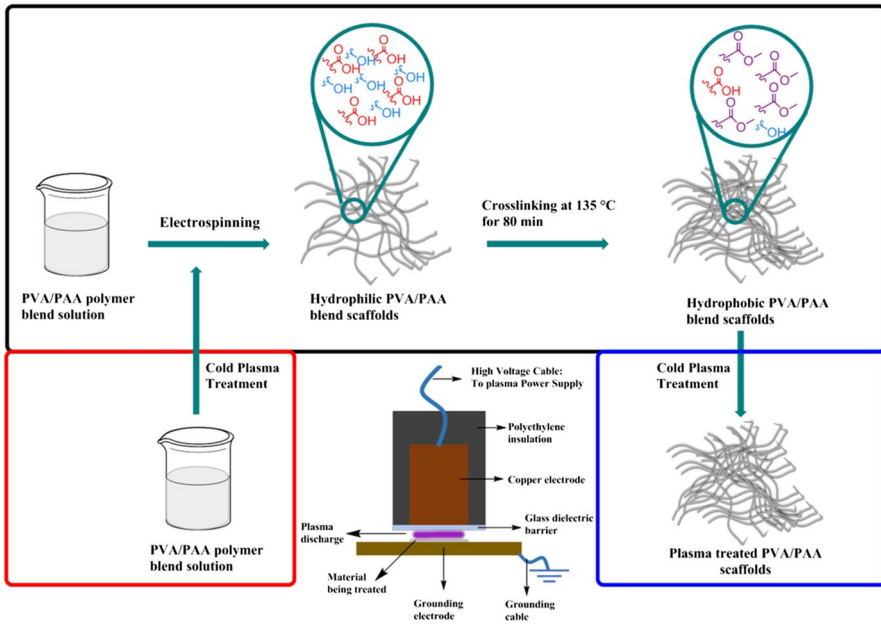


Fig. 1 Schematic of the preparation of PVA/PAA scaffolds and CAP modification

fixed to 10 min to ensure equal thickness. The relative humidity and temperature were 55% and 26 °C, respectively. Both random and aligned nanofibers were collected using stationary and rotating drum collectors. The resulting PVA/PAA nanofibers were cross-linked via heat treatment at 135 °C for 80 min to obtain water-stable scaffolds. The third set of electrospun PVA/PAA scaffolds was treated with CAP (PT-nanofibers) for 1, 3, and 5 min.

Characterization methods

Morphology of the electrospun PVA/PAA nanofibers was observed using a scanning electron microscope (SEM) (Carl Zeiss 300VP, Germany). The fiber diameter distributions were estimated statistically based on SEM micrographs using ImageJ software (NIH, Bethesda, MD, USA). The static contact angles of the nanofibers were measured using the sessile drop method with a KSV Attension Theta Lite Optical Tensiometer. For each sample, a 4.5 μL drop of DW was used on the nanofiber surface and then averaged three independent measurements. Fourier-transform infrared (FTIR) spectra were registered in a Perkin Elmer Spectrum 100 spectrometer with a spectral resolution of 4 cm^{-1} . Polarization of the incident IR radiation was achieved with a ZnSe polarizer.

Antimicrobial activity of the CAP-treated electrospun PVA/PAA scaffold was tested using the *E. coli* ATCC 25922 strain. Briefly, 1 mL of frozen stock of *E. coli* ATCC 25922 was transferred into 9 mL of TSB and incubated it overnight in

a shaker incubator at 37 °C and 200 rpm. After overnight incubation microbial concentration was set to 10^6 CFU/mL. Hundred microliters of 10^6 CFU/mL *E. coli* ATCC 25922 was transferred onto $1\text{ cm}^2 \times 1\text{ cm}^2$ plasma-treated electrospun PVA scaffolds, where they remained for 30 min. Then, 1 mL of sterile 1X PBS was added and scaffolds were gently agitated to homogenize the bacteria, serial dilutions were made, and bacteria were plated on TSA plates and incubated for 24 h at 37 °C. After incubation, surviving colonies were counted and expressed as \log_{10} surviving colonies.

For the in vitro wound scratch test assay, the fabricated nanofibers were covered with fresh sterile medium (at a 4 g/20 mL ratio) and were extracted at 37 °C for 24 h. L929 mouse fibroblasts were seeded on 24-well plates at a density of 5×10^4 cells/cm² and allowed 24 h to enable cell adhesion and the formation of a confluent monolayer at 37 °C and 5% CO₂. Confluent monolayers were scored with sterile 200- μ L pipette tips to leave wounds approximately 0.4–0.5 mm in width. Culture medium was then immediately removed and rinsed with PBS to clean off any cellular debris. Removed medium was replaced with fresh media (for the control group) and extract media for the groups of DW, PT–DW, PT, and control groups. Next, the extract was subjected on the cells for 24 h. The in vitro wound scratch closure was monitored and images were captured with an Olympus CKX41 inverted microscope (Olympus, Tokyo, Japan) at 0, 24, 48, and 72 h. The percentage of healed wound areas for the DW, PT–DW, PT, and control groups at each time point was analyzed by using ImageJ software. All scratch assays were performed in triplicate. Significant differences between the groups were evaluated using a two-tailed student's *t* test. A value of $p < 0.05$ was considered statistically significant.

Results and discussion

The uniformity of electrospun nanofibers depends not only on the process parameters but also on the properties of the polymer solution. In this work, uniform, bead-free, and water-stable PVA/PAA nanofibers were successfully fabricated. The water stability of the fibrous scaffolds was obtained by thermal treatment at a temperature of 135 °C for 80 min, during which cross-linking occurs between the hydroxyl groups of PVA and the carboxyl groups of PAA [31] (see FTIR analysis in Fig. S1, Supporting Information). The thermal cross-linking brought remarkable water resistivity, while maintaining the fibrous structures of the scaffolds even after immersion in water for months (see Fig. S2, Supporting Information). CAP treatment of the medium results increased in conductivity, viscosity, and surface tension [5]. To investigate the effect of CAP treatment, electrospinning solutions of PVA/PAA were prepared by using DW and PT–DW. However, CAP treatment of the polymer solution could not be achieved for this study because of the surface cross-linking that occurred due to the generation of oxygen-containing species during the plasma process [32]. Therefore, the electrospun polymer scaffolds obtained from DW were subjected to different plasma exposure times (PT).

Morphology of electrospun PVA/PAA nanofiber scaffolds

Figure 2 shows SEM micrographs of both untreated and CAP-treated scaffolds, and the variation in the fiber diameter with respect to plasma exposure time. A relative decrease in the average fiber diameter from 220 ± 20 to 170 ± 20 nm was observed, associated with an increase in the treatment time from 0 to 5 min. A possible explanation for the decrease in the fiber diameter is the diffusion of etching species generated during the CAP treatment, which transfers the energy of the incoming ions to the reactive species [33]. Furthermore, CAP treatment resulted in no significant alteration in the surface morphology of the nanofibers. Nor did we observe any degradation or agglomeration of/between the nanofibers. Figure 3 shows SEM micrographs of the nanofibers, in which we can see changes in diameter with both the

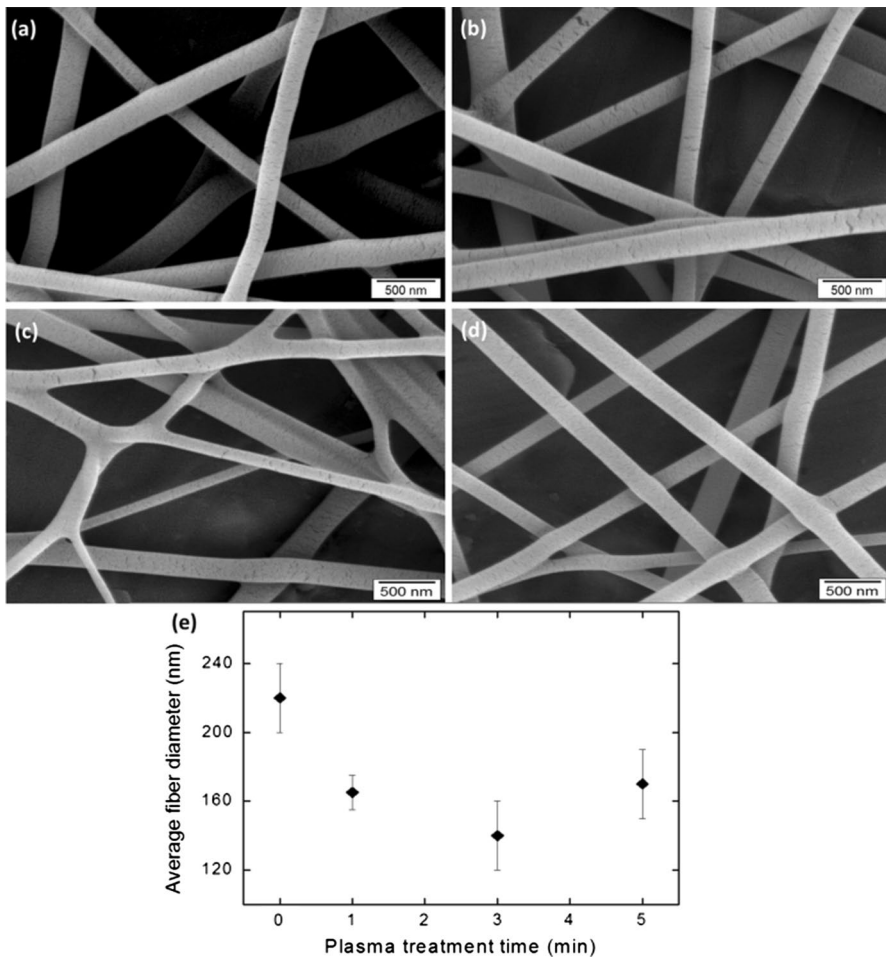


Fig. 2 SEM micrographs of random PVA/PAA nanofibers **a** untreated; CAP-treated for **b** 1 min, **c** 3 min, and **d** 5 min; and **e** variation of average fiber diameter with respect to the treatment time

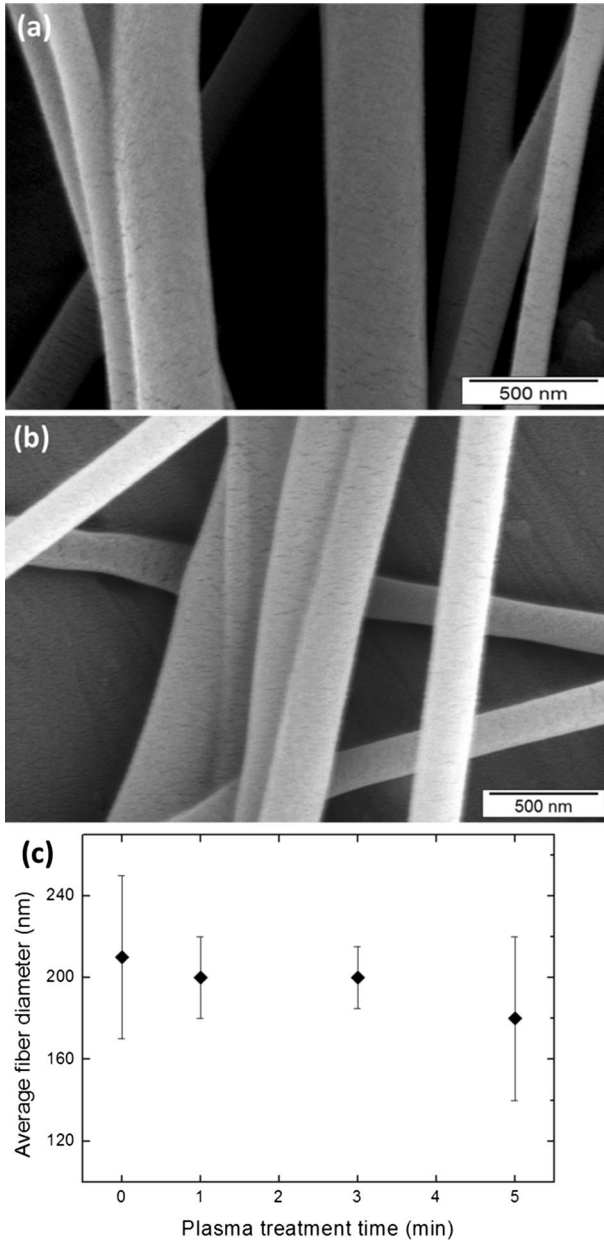


Fig. 3 SEM micrographs of aligned PVA/PAA nanofibers **a** untreated, CAP-treated for **b** 3 min; and **c** variation in the average fiber diameter with respect to treatment time

alignment of the nanofibers and CAP treatment times. The average fiber diameter of the aligned nanofibers was 210 ± 40 nm. After CAP treatment, the size of the nanofibers relatively decreased to 180 ± 40 nm. Although we observed a similar

trend in the aligned and random fibers, the trend in the aligned fibers was insignificant compared with that of the random fibers.

Table 1 lists the contact angle values of the random and aligned nanofibrous scaffolds, in which we can see that the contact angles obtained for the random and aligned PVA/PAA scaffolds were 62 ± 6.0 and 73 ± 8.0 , respectively. This indicates that fiber alignment has no significant effect on surface hydrophilicity. On the other hand, after only 3 min of CAP treatment, the contact angle values of the scaffolds decreased (by 40%) regardless of the fiber alignment. The reduction in contact angle of the scaffolds indicates higher hydrophilicity on the surface of the scaffolds, which can be explained by a flux of reactive oxygen or nitrogen species onto the fiber surfaces [30].

The morphology, in terms of molecular orientation, of PVA/PAA under an electrical field and CAP treatment was also investigated by polarized FTIR spectroscopy. Figure 4 shows the polarized FTIR spectra of untreated and CAP-treated random (DW-r, PT-r) and aligned (DW-a, PT-a) PVA/PAA nanofibers. The spectrum of PVA/PAA nanofibers is consistent with that reported in the literature [31]. The FTIR spectra of all the nanofiber samples showed characteristic peak absorptions: a broad band at around 3345 cm^{-1} (O–H stretching), a band at 2942 cm^{-1} (C–H stretching), a sharp band at 1718 cm^{-1} (C=O stretching), and a double band at around $1000\text{--}1300 \text{ cm}^{-1}$ (C–O stretching). Generally, the increment of IR radiation intensity of the bands was observed with the formation of ionic species upon CAP treatment (see Fig. S3, Supporting Information).

The parallel and perpendicularly polarized spectra of the random fibers (DW-r) are almost identical, which indicates that there is no preferential alignment of the polymer chains. However, in both the aligned and CAP-treated fibers, the absorbance values of the parallel and perpendicularly polarized FTIR spectra are remarkably different. The intensities of the vibrational bands undergo change depending on the polarization of the incident IR beam. The difference in the absorbance values of the random and uniaxially aligned PVA fibers as evidence of chain alignment within the fibers has been reported [34]. Furthermore, the effect of CAP treatment on the alignment of the nanofibers was investigated. The degree of alignment of electrospun polymer chains can be quantified by their dichroic ratio (R), which is the ratio of the absorption intensity of the parallel component with respect to that of the perpendicular component ($R = A_{\parallel}/A_{\perp}$). We took into consideration the vibrational bands at 2942 and 1097 cm^{-1} , which correspond to the stretching of the methylene ($-\text{CH}_2$) units on the backbone (parallel to the fiber axis) and CO units (perpendicular to the fiber axis), respectively. The dichroic ratios for the bands at 2942 and 1097 cm^{-1}

Table 1 Contact angle comparison of the fibers before and after CAP treatment for 3 min

	Contact angle ($^{\circ}$) for PVA/PAA fibers	
	Random	Aligned
DW	62 ± 6.0	73 ± 8.0
PT-nanofibers	37 ± 4.0	44 ± 6.0

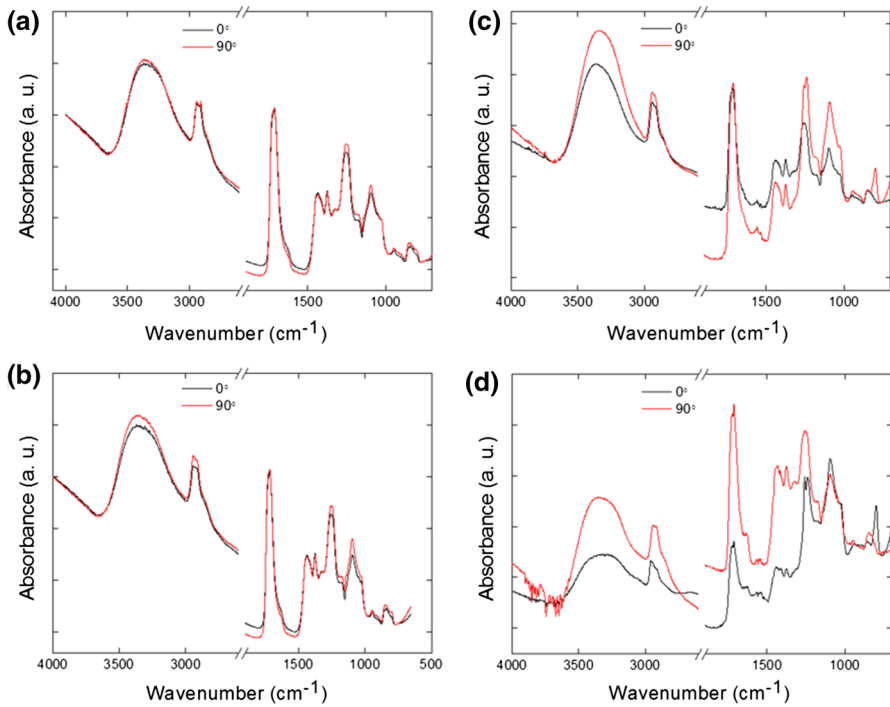
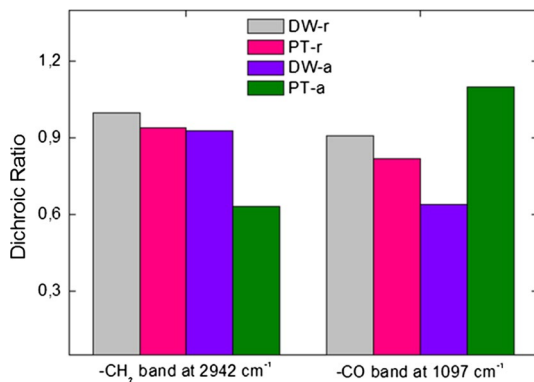


Fig. 4 Polarized FTIR spectra of untreated and CAP-treated random **a** DW-r, **b** PT-r, and aligned **c** DW-a, **d** PT-a PVA/PAA nanofibers

are shown in Fig. 5. The oxygen-linked pendant groups of the PVA (CO) seem to be more aligned in the PT-a samples. Not only the high extensional force generated by electrospinning but also the formation of reactive species on the fibers during plasma treatment alters the chain alignment indicating the changes in surface chemistry. On the other hand, the lower dichroic ratio of electrospun PVA/PAA fibers compared to other polymeric fibers reported in the literature [35, 36] may be related

Fig. 5 Dichroic ratios of the bands at 2942 and 1096 cm⁻¹ for the PVA/PAA nanofibers



to the partial cross-linking of PVA and PAA due to the formation of hydrogen bonds. We also considered that the alignment of polymer chains by the manipulation of the electrical field using a rotating drum and the elongational force generated by electrospinning could perpendicularly orient the functional groups to the fiber surfaces, which may contribute to the further alignment during CAP treatment through the formation of reactive species on the fibers.

CAP treatment is an emerging application that has drawn much attention for its use in biomedical applications due to its ability to develop antibacterial and biocompatible scaffolds without changing the physical and mechanical properties of electrospun nanofibrous scaffolds [37, 38]. Antimicrobial activity of the DW, PT–DW, and PT groups was evaluated in a colony counting assay. As demonstrated in Fig. 6, a 5-log bacterial reduction was achieved in the random and aligned scaffolds of the PT group, whereas the bacterial reduction was less than 1 log in the

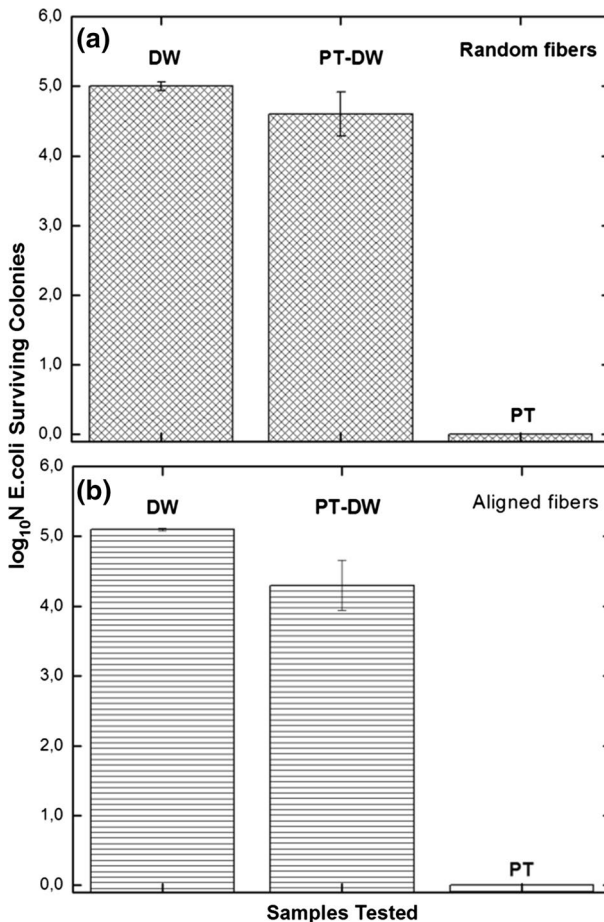


Fig. 6 Antimicrobial activities of **a** random and **b** aligned electrospun scaffolds. CAP-treated random and aligned scaffolds demonstrated capability of 5-log inactivation of *E. coli*

random and aligned scaffolds of the PT–DW group. The results indicate that the antimicrobial effect is independent of fiber alignment. The antimicrobial effect of nonthermal atmospheric plasmas in broad spectrum microorganisms is well documented [39]. Furthermore, liquids and gels might demonstrate strong antimicrobial activity when treated with nonthermal plasma [19, 40]. Reactive oxygen and nitrogen species (ROS and RNS), generated during the formation of plasma, and their reaction with treated material have been correlated with antimicrobial activity [41]. The antimicrobial effect in the PT group could be attributed to the accumulation of plasma-generated species and the chemical modification of the scaffold surface. The loss of antimicrobial activity in the PT–DW group was ascribed to the quenching of the plasma-generated ROS and RNS upon mixing CAP-treated water with PVA powder. Either the surrounding environment and/or the addition of untreated substances to a CAP-treated substance could scavenge plasma-generated chemical species that are responsible for the antimicrobial effect, as previously reported elsewhere [42]. Plasma-generated ROS and RNS are highly reactive and were possibly consumed in the structural alteration of PVA upon mixing it with CAP-treated water; sufficient concentration of those species to achieve antimicrobial activity could not be reached. However, the reaction of plasma-generated species with PVA/PAA caused a reduction in the contact angle following electrospinning in the PT–DW group. Previously, de Avila et al. [43] and İbiş et al. [44] reported decreased bacterial adhesion on various surfaces with increased hydrophilicity after UV photofunctionalization and CAP treatment. Therefore, increased hydrophilicity could also have contributed to the antimicrobial activity in the PT group. In more detail, the chemical modification of CAP-treated materials mainly involves the addition of polar groups such as hydroxyl groups, which subsequently leads to increased hydrophilicity, which is consistent with the findings in this study. The increased hydrophilicity of CAP-treated materials prevents bacterial adhesion and subsequently prevents microbial growth [10, 44, 45]. Furthermore, the CAP-treatment-dependent accumulation of reactive oxygen and nitrogen species (RONS) causes change in the surface charge of treated material, which might induce an electrostatic interaction between the material and bacteria, thereby causing permeabilization of the cell membrane and eventual bacterial inactivation [46].

The micrographs of in vitro scratch assays at 0, 24, 48, and 72 h for the DW, PT–DW, PT, and control groups are demonstrated in Fig. 7A1–A4, B1–B4, C1–C4, and D1–D4, respectively. Figure 7E shows the percentages of the healed wound area in the DW, PT–DW, PT, and control groups at each time point. The wound area at time 0 on the regular polystyrene culture wells was used as the control, and for each time point (24, 48, and 72 h) wound closure was calculated. As shown in the 0-h micrographs of the DW, PT–DW, PT, and control groups, the in vitro wounds were uniformly formed. We observed that close to 80% of the scratched areas tended to heal within 72 h. Moreover, compared to the control group, we found the wound repair ability to be significantly higher in the DW ($p < 0.05$), PT–DW ($p < 0.001$), and PT ($p < 0.01$) groups at 72 h. For instance, at 72 h, the control group occupied a 69.9 ± 2.4 wound area, whereas the DW, PT–DW, and PT groups occupied 79.9 ± 1.1 , 82.5 ± 1.2 , and 76.7 ± 0.8 , respectively. Similarly, Dolci et al. [47] demonstrated that CAP treatment on poly(L-lactic acid) (PLLA) electrospun nanofibers

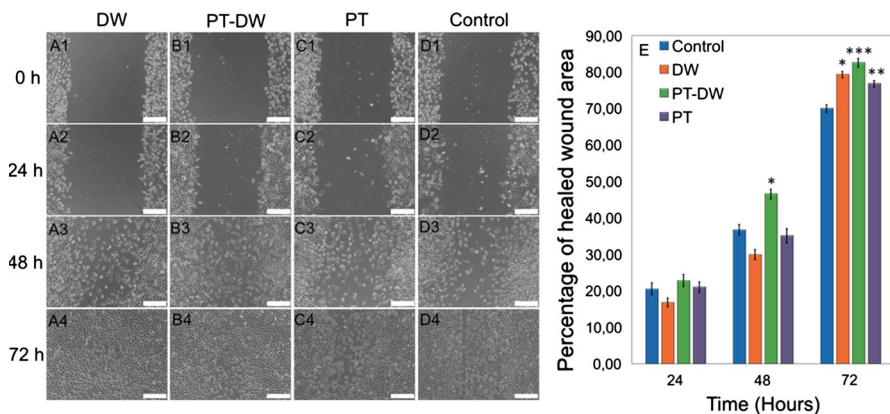


Fig. 7 In vitro scratch assays of **a** DW, **b** PT–DW, **c** PT, and **d** control at 0, 24, 48, and 72 h. The percentages of healed wound areas for DW, PT–DW, PT, and control groups at each time point (**e**)

significantly enhanced mouse fibroblast viability compared to untreated PLLA nanofibers. In another study, Atyabi et al. [48] reported that CAP treatment provided a superior surface for L929 mouse fibroblasts on poly(ϵ -caprolactone) (PCL) nanofibers. The accumulation and release of CAP-generated RONS, along with the chemical modification of the treated material, are thought to be the primary sources of enhanced biocompatibility and/or increased cell proliferation [19, 38, 49]. Another potential reason for the enhanced biocompatibility is that CAP treatment significantly increases the hydrophilicity of electrospun scaffolds, which sharply promotes cellular adhesion and proliferation [38]. In addition, oxygen-containing charged species that are formed on the surface of the electrospun scaffolds may enhance the adsorption of integrin-binding protein and be directly correlated with increased cell adhesion and proliferation [50, 51]. In a recent study, Karaman et al. [52] demonstrated that CAP treatment on titanium surfaces significantly increased the adhesion and proliferation of mesenchymal stem cells.

Conclusions

In this study, we examined the effects of cold atmospheric plasma (CAP) treatment on random and aligned electrospun polyvinyl alcohol (PVA)/polyacrylic acid (PAA) nanofibers. The surface properties of PVA/PAA nanofibers after CAP treatment showed remarkable changes without sustaining any damage to their morphologies. Depending on the plasma exposure time, the average diameter of both random and aligned fibers relatively decreased. After only 3 min of CAP treatment, the contact angle values of the nanofiber scaffolds decreased and showed improvement in surface wettability. Using the vibrational polarization spectroscopy, we observed the stretching of charged polymer chains in the electrical field direction during electrospinning and CAP. Both the extensional force caused by the electrostatic field during directed electrospinning and the generation of oxygen-rich species by CAP

treatment induce chain alignment along the fiber axis. Moreover, antimicrobial tests have shown that electrospun PVA/PAA scaffolds can acquire strong antibacterial activity when treated with CAP. It was also observed in in vitro scratch assays that CAP treatment on PVA/PAA fibers had no toxic effect on the fibers. The proposed strategy for the plasma surface modification of electrospun nanofibers may break new ground for various biomedical applications.

Acknowledgements The authors thank the Centre for Materials Research of Izmir Katip Celebi University (IKCU). Partial financial support for this research was provided by the IKCU Scientific Research Project 2014-1-MÜH-15.

References


1. Ma PX (2004) Scaffolds for tissue fabrication. *Mater Today* 7(5):30–40. [https://doi.org/10.1016/s1369-7021\(04\)00233-0](https://doi.org/10.1016/s1369-7021(04)00233-0)
2. Bazaka K, Jacob MV, Chrzanowski W, Ostrikov K (2015) Anti-bacterial surfaces: natural agents, mechanisms of action, and plasma surface modification. *RSC Adv* 5(60):48739–48759. <https://doi.org/10.1039/c4ra17244b>
3. Ulbin-Figlewicz N, Brychey E, Jarmoluk A (2015) Effect of low-pressure cold plasma on surface microflora of meat and quality attributes. *J Food Sci Technol* 52(2):1228–1232. <https://doi.org/10.1007/s13197-013-1108-6>
4. Padil VVT, Nguyen NHA, Rozek Z, Sevcu A, Cernik M (2015) Synthesis, fabrication and anti-bacterial properties of a plasma modified electrospun membrane consisting of gum kondagogu, dodeceny succinic anhydride and poly(vinyl alcohol). *Surf Coat Technol* 271:32–38. <https://doi.org/10.1016/j.surfcoat.2015.01.035>
5. Shi QA, Vitichuli N, Nowak J, Lin Z, Guo BK, McCord M, Bourham M, Zhang XW (2011) Atmospheric plasma treatment of pre-electrospinning polymer solution: a feasible method to improve electrospinnability. *J Polym Sci Part B Polym Phys* 49(2):115–122. <https://doi.org/10.1002/polb.22157>
6. Nawalakhe R, Shi Q, Vitichuli N, Bourham MA, Zhang XW, McCord MG (2015) Plasma-assisted preparation of high-performance chitosan nanofibers/gauze composite bandages. *Int J Polym Mater Polym Biomater* 64(14):709–717. <https://doi.org/10.1080/00914037.2014.1002098>
7. Nawalakhe R, Shi Q, Vitichuli N, Noar J, Caldwell JM, Breidt F, Bourham MA, Zhang X, McCord MG (2013) Novel atmospheric plasma enhanced chitosan nanofiber/gauze composite wound dressings. *J Appl Polym Sci* 129(2):916–923. <https://doi.org/10.1002/app.38804>
8. Silva SS, Luna SM, Gomes ME, Benesch J, Pashkuleva I, Mano JF, Reis RL (2008) Plasma surface modification of chitosan membranes: characterization and preliminary cell response studies. *Macromol Biosci* 8(6):568–576. <https://doi.org/10.1002/mabi.200700264>
9. Theapsak S, Watthanaphanit A, Rujiravanit R (2012) Preparation of chitosan-coated polyethylene packaging films by DBD plasma treatment. *ACS Appl Mater Interfaces* 4(5):2474–2482. <https://doi.org/10.1021/am300168a>
10. Yorsaeng S, Pornsunthorntawe O, Rujiravanit R (2012) Preparation and characterization of chitosan-coated DBD plasma-treated natural rubber latex medical surgical gloves with antibacterial activities. *Plasma Chem Plasma Process* 32(6):1275–1292. <https://doi.org/10.1007/s11090-012-9405-9>
11. Nhi TT, Khon HC, Hoai NTT, Bao BC, Quyen TN, Toi VV, Hiep NT (2016) Fabrication of electrospun polycaprolactone coated with chitosan-silver nanoparticles membranes for wound dressing applications. *J Mater Sci Mater Med* 27(10):156. <https://doi.org/10.1007/s10856-016-5768-4>
12. Siri S, Wadbua P, Amornkitbamrung V, Kampa N, Maensiri S (2010) Surface modification of electrospun PCL scaffolds by plasma treatment and addition of adhesive protein to promote fibroblast cell adhesion. *Mater Sci Technol* 26(11):1292–1297. <https://doi.org/10.1179/026708310x12798718274070>

13. Suwanton O (2016) Biomedical applications of electrospun polycaprolactone fiber mats. *Polym Adv Technol* 27(10):1264–1273. <https://doi.org/10.1002/pat.3876>
14. Jacobs T, Declercq H, De Geyter N, Cornelissen R, Dubruel P, Leys C, Beaurain A, Payen E, Morent R (2013) Plasma surface modification of polylactic acid to promote interaction with fibroblasts. *J Mater Sci Mater Med* 24(2):469–478. <https://doi.org/10.1007/s10856-012-4807-z>
15. Zhu W, Castro NJ, Cheng XQ, Keidar M, Zhang LG (2015) Cold atmospheric plasma modified electrospun scaffolds with embedded microspheres for improved cartilage regeneration. *PLoS ONE* 10(7):e0134729. <https://doi.org/10.1371/journal.pone.0134729>
16. Padil VVT, Cernik M (2015) Poly(vinyl alcohol)/gum karaya electrospun plasma treated membrane for the removal of nanoparticles (Au, Ag, Pt, CuO and Fe₃O₄) from aqueous solutions. *J Hazard Mater* 287:102–110. <https://doi.org/10.1016/j.jhazmat.2014.12.042>
17. Chen JP, Chiang Y (2010) Bioactive electrospun silver nanoparticles-containing polyurethane nanofibers as wound dressings. *J Nanosci Nanotechnol* 10(11):7560–7564. <https://doi.org/10.1166/jnn.2010.2829>
18. Chen HN, Xing XD, Tan HP, Jia Y, Zhou TL, Chen Y, Ling ZH, Hu XH (2017) Covalently antibacterial alginate-chitosan hydrogel dressing integrated gelatin microspheres containing tetracycline hydrochloride for wound healing. *Mater Sci Eng C Mater Biol Appl* 70:287–295. <https://doi.org/10.1016/j.msec.2016.08.086>
19. Poor AE, Ercan UK, Yost A, Brooks AD, Joshi SG (2014) Control of multi-drug-resistant pathogens with non-thermal-plasma-treated alginate wound dressing. *Surg Infect* 15(3):233–243. <https://doi.org/10.1089/sur.2013.050>
20. Furusho H, Kitano K, Hamaguchi S, Nagasaki Y (2009) Preparation of stable water-dispersible PEGylated gold nanoparticles assisted by nonequilibrium atmospheric-pressure plasma jets. *Chem Mater* 21(15):3526–3535. <https://doi.org/10.1021/cm803290b>
21. Dorraki N, Safa NN, Jahanfar M, Ghomi H, Ranaei-Siadat SO (2015) Surface modification of chitosan/PEO nanofibers by air dielectric barrier discharge plasma for acetylcholinesterase immobilization. *Appl Surf Sci* 349:940–947. <https://doi.org/10.1016/j.apsusc.2015.03.118>
22. Liu W, Zhan JC, Su Y, Wu T, Wu CC, Ramakrishna S, Mo XM, Al-Deyab SS, El-Newehy M (2014) Effects of plasma treatment to nanofibers on initial cell adhesion and cell morphology. *Colloids Surf B Biointerfaces* 113:101–106. <https://doi.org/10.1016/j.colsurfb.2013.08.031>
23. Horzum N, Boyaci E, Eroglu AE, Shahwan T, Demir MM (2010) Sorption efficiency of chitosan nanofibers toward metal ions at low concentrations. *Biomacromol* 11(12):3301–3308. <https://doi.org/10.1021/bm100755x>
24. Horzum N, Mari M, Wagner M, Fortunato G, Popa AM, Demir MM, Landfester K, Crespy D, Munoz-Espi R (2015) Controlled surface mineralization of metal oxides on nanofibers. *RSC Adv* 5(47):37340–37345. <https://doi.org/10.1039/c5ra02140e>
25. Dolci LS, Quiroga SD, Gherardi M, Laurita R, Liguori A, Sanibondi P, Fiorani A, Calza L, Colombo V, Focarete ML (2014) Carboxyl surface functionalization of poly(L-lactic acid) electrospun nanofibers through atmospheric non-thermal plasma affects fibroblast morphology. *Plasma Process Polym* 11(3):203–213. <https://doi.org/10.1002/ppap.201300104>
26. Park SJ, Rhee KY, Jin FL (2015) Improvement of hydrophilic properties of electrospun polyamide-imide fibrous mats by atmospheric-pressure plasma treatment. *J Phys Chem Solids* 78:53–58. <https://doi.org/10.1016/j.jpcs.2014.11.001>
27. Ozkan O, Sasmazel HT (2016) Effects of nozzle type atmospheric dry air plasma on L929 fibroblast cells hybrid poly(ϵ -caprolactone)/chitosan/poly(ϵ -caprolactone) scaffolds interactions. *J Biosci Bioeng* 122(2):232–239. <https://doi.org/10.1016/j.jbiosc.2016.01.004>
28. Colombo V, Fabiani D, Focarete ML, Gherardi M, Gualandi C, Laurita R, Zaccaria M (2014) Atmospheric pressure non-equilibrium plasma treatment to improve the electrospinnability of poly(L-lactic acid) polymeric solution. *Plasma Process Polym* 11(3):247–255. <https://doi.org/10.1002/ppap.201300141>
29. Kumeta K, Nagashima I, Matsui S, Mizoguchi K (2003) Crosslinking reaction of poly(vinyl alcohol) with poly(acrylic acid) (PAA) by heat treatment: effect of neutralization of PAA. *J Appl Polym Sci* 90(9):2420–2427. <https://doi.org/10.1002/app.12910>
30. Ercan UK, Wang H, Ji HF, Fridman G, Brooks AD, Joshi SG (2013) Nonequilibrium plasma-activated antimicrobial solutions are broad-spectrum and retain their efficacies for extended period of time. *Plasma Process Polym* 10(6):544–555. <https://doi.org/10.1002/ppap.201200104>
31. Xiao SL, Shen MW, Guo R, Huang QG, Wang SY, Shi XY (2010) Fabrication of multi-walled carbon nanotube-reinforced electrospun polymer nanofibers containing zero-valent iron

- nanoparticles for environmental applications. *J Mater Chem* 20(27):5700–5708. <https://doi.org/10.1039/c0jm00368a>
32. Audic JL, Poncin-Epaillard F, Reyx D, Brosse JC (2001) Cold plasma surface modification of conventionally and nonconventionally plasticized poly(vinyl chloride)-based flexible films: global and specific migration of additives into isooctane. *J Appl Polym Sci* 79(8):1384–1393. [https://doi.org/10.1002/1097-4628\(20010222\)79:8<1384::aid-app50>3.0.co;2-h](https://doi.org/10.1002/1097-4628(20010222)79:8<1384::aid-app50>3.0.co;2-h)
 33. Verdonck P, Caliope PB, Hernandez ED, da Silva ANR (2006) Plasma etching of electrospun polymeric nanofibres. *Thin Solid Films* 515(2):831–834. <https://doi.org/10.1016/j.tsf.2005.12.196>
 34. Demir MM, Ozen B, Ozelcik S (2009) Formation of pseudoisocyanine J-aggregates in poly(vinyl alcohol) fibers by electrospinning. *J Phys Chem B* 113(34):11568–11573. <https://doi.org/10.1021/jp902380n>
 35. Nobeshima T, Sakai H, Ishii Y, Uemura S, Yoshida M (2016) Polarized FT-IR study of uniaxially aligned electrospun poly(DL-lactic acid) fiber films. *J Photopolym Sci Technol* 29(2):353–356. <https://doi.org/10.2494/photopolymer.29.353>
 36. Ramazani S, Karimi M (2014) Investigating the influence of temperature on electrospinning of polycaprolactone solutions. *E-Polymers* 14(5):323–333. <https://doi.org/10.1515/epoly-2014-0110>
 37. Wang M, Cheng X, Zhu W, Holmes B, Keidar M, Zhang LG (2014) Design of biomimetic and bioactive cold plasma-modified nanostructured scaffolds for enhanced osteogenic differentiation of bone marrow-derived mesenchymal stem cells. *Tissue Eng Part A* 20(5–6):1060–1071. <https://doi.org/10.1089/ten.TEA.2013.0235>
 38. Zhu W, Castro NJ, Cheng X, Keidar M, Zhang LG (2015) Cold atmospheric plasma modified electrospun scaffolds with embedded microspheres for improved cartilage regeneration. *PLoS ONE* 10(7):e0134729. <https://doi.org/10.1371/journal.pone.0134729>
 39. Moreau N, Orange N, Feuilloley M (2008) Non-thermal plasma technologies: new tools for bio-decontamination. *Biotechnol Adv* 26(6):610–617. <https://doi.org/10.1016/j.biotechadv.2008.08.001>
 40. Traylor MJ, Pavlovich MJ, Karim S, Hait P, Sakiyama Y, Clark DS, Graves DB (2011) Long-term antibacterial efficacy of air plasma-activated water. *J Phys D Appl Phys* 44(47):472001. <https://doi.org/10.1088/0022-3727/44/47/472001>
 41. Ercan UK, Smith J, Ji H-F, Brooks AD, Joshi SG (2016) Chemical changes in nonthermal plasma-treated N-acetylcysteine (NAC) solution and their contribution to bacterial inactivation. *Sci Rep* 6:20365. <https://doi.org/10.1038/srep20365>
 42. Ryu Y-H, Kim Y-H, Lee J-Y, Shim G-B, Uhm H-S, Park G, Choi EH (2013) Effects of background fluid on the efficiency of inactivating yeast with non-thermal atmospheric pressure plasma. *PLoS ONE* 8(6):e66231. <https://doi.org/10.1371/journal.pone.0066231>
 43. de Avila ED, Lima BP, Sekiya T, Torii Y, Ogawa T, Shi W, Lux R (2015) Effect of UV-photo-functionalization on oral bacterial attachment and biofilm formation to titanium implant material. *Biomaterials* 67:84–92. <https://doi.org/10.1016/j.biomaterials.2015.07.030>
 44. Ibis F, Oflaz H, Ercan UK (2016) Biofilm inactivation and prevention on common implant material surfaces by nonthermal DBD plasma treatment. *Plasma Med* 6(1):33–45. <https://doi.org/10.1615/PlasmaMed.2016015846>
 45. Monetta T, Scala A, Malmo C, Bellucci F (2011) Antibacterial activity of cold plasma-treated titanium alloy. *Plasma Med* 1(3–4):205–214. <https://doi.org/10.1615/PlasmaMed.v1.i3-4.30>
 46. Liguori A, Cochis A, Stancampiano A, Laurita R, Azzimonti B, Sorrentino R, Varoni EM, Petri M, Colombo V, Gherardi M, Rimondini L (2017) Cold atmospheric plasma treatment affects early bacterial adhesion and decontamination of soft relined palatal obturators. *Clin Plasma Med* 7:36–45. <https://doi.org/10.1016/j.cpme.2017.08.001>
 47. Dolci LS, Quiroga SD, Gherardi M, Laurita R, Liguori A, Sanibondi P, Fiorani A, Calzà L, Colombo V, Focarete ML (2014) Carboxyl surface functionalization of poly(L-lactic acid) electrospun nanofibers through atmospheric non-thermal plasma affects fibroblast morphology. *Plasma Process Polym* 11(3):203–213. <https://doi.org/10.1002/ppap.201300104>
 48. Atyabi SM, Sharifi F, Irani S, Zandi M, Mivehchi H, Nagheh Z (2016) Cell attachment and viability study of PCL nano-fiber modified by cold atmospheric plasma. *Cell Biochem Biophys* 74(2):181–190. <https://doi.org/10.1007/s12013-015-0718-1>
 49. Kasálková N, Makajová Z, Pařízek M, Slepíčka P, Kolářová K, Bačáková L, Hnatowicz V, Švorčík V (2010) Cell adhesion and proliferation on plasma-treated and poly(ethylene

- glycol)-grafted polyethylene. *J Adhes Sci Technol* 24(4):743–754. <https://doi.org/10.1163/016942409X12579497420762>
50. Kim CH, Khil MS, Kim HY, Lee HU, Jahng KY (2006) An improved hydrophilicity via electrospinning for enhanced cell attachment and proliferation. *J Biomed Mater Res Part B Appl Biomater* 78(2):283–290. <https://doi.org/10.1002/jbm.b.30484>
 51. Moffa M, Polini A, Sciancalepore AG, Persano L, Mele E, Passione LG, Potente G, Pisignano D (2013) Microvascular endothelial cell spreading and proliferation on nanofibrous scaffolds by polymer blends with enhanced wettability. *Soft Matter* 9(23):5529–5539. <https://doi.org/10.1039/C3SM50328C>
 52. Karaman O, Kelebek S, Demirci EA, İbiş F, Ulu M, Ercan UK (2018) Synergistic effect of cold plasma treatment and RGD peptide coating on cell proliferation over titanium surfaces. *Tissue Eng Regen Med* 15(1):13–24. <https://doi.org/10.1007/s13770-017-0087-5>

Affiliations

Nehir Arik¹ · Alper Inan² · Fatma Ibiş³ · Emine A. Demirci³ · Ozan Karaman^{3,4} · Utku K. Ercan^{3,4} · Nesrin Horzum^{1,5} 

Nehir Arik
nhrark@gmail.com

Alper Inan
alperinan@std.iyte.edu.tr

Fatma Ibiş
fatmaibiss@gmail.com

Emine A. Demirci
afrademirci@gmail.com

Ozan Karaman
ozan.karaman@ikc.edu.tr

Utku K. Ercan
utkuk.ercan@ikc.edu.tr

¹ Biocomposite Engineering Graduate Program, İzmir Katip Celebi University, İzmir 35620, Turkey

² Department of Chemistry, İzmir Institute of Technology, İzmir 35430, Turkey

³ Biomedical Technologies Graduate Program, İzmir Katip Celebi University, İzmir 35620, Turkey

⁴ Department of Biomedical Engineering, İzmir Katip Celebi University, İzmir 35620, Turkey

⁵ Department of Engineering Sciences, İzmir Katip Celebi University, İzmir 35620, Turkey